Structure of porous Vycor glass

P. Wiltzius, F. S. Bates, and S. B. Dierker

AT&T Bell Laboratories, Murray Hill, New Jersey 07974

G. D. Wignall

Oak Ridge National Laboratory, Oak Ridge, Tennessee 37830
(Received 8 May 1987)

Small-angle neutron scattering experiments investigating the structure of porous Vycor glass are reported. The long-wave-length behavior $(0.004 \text{ Å}^{-1} \leq q \leq 0.025 \text{ Å}^{-1})$ of the measured structure factor $S(q)$ is in good agreement with Cahn's prediction for spinodal decomposition. The high-q data do not conclusively establish whether the internal surfaces are fractally rough over the length scales probed. Experiments on Vycor contrasted with protonated and deuterated cyclohexane reveal local composition gradients within the glass.

Porous media have enjoyed increased popularity as host structures for the study of a variety of physical phenomena such as hydrodynamic flow,[1-4] viscous fingering and interfacial instability,[5,6] diffusion,[7,8] supercooling of liquids,[9] electronic energy transfer,[10-12] superfluidity in Bose gases,[13,14] and critical phenomena in binary fluid mixtures.[15,16] An issue of particular interest is the crossover from translational invariance to self-similarity as the length scales involved change. The structure of various porous networks and the associated internal surfaces have been proposed[7,10,11] to have fractal geometry, although little direct structural evidence has been presented. The commercially available porous Vycor glass (Vycor 7930, Dow Corning) has been used in some of the above-mentioned studies. Here we report the results of a quantitative evaluation of the structure of Vycor by means of the small-angle neutron scattering (SANS) technique.

Vycor is manufactured from a borosilicate glass-forming melt with a high concentration of B_2O_3. This melt is cooled below its demixing temperature forcing it to spinodally decompose into a SiO_2-rich phase and a B_2O_3-alkali oxide-rich phase. The latter is acid soluble and can be leached out with suitable solvents leaving a fully penetrable microporous glass. Because of its large internal surface area, organic materials are readily absorbed from the surrounding atmosphere. Prior to using Vycor we subjected it to a cleaning procedure with hydrogen peroxide followed by drying under a nitrogen atmosphere. The cleaned glass was colorless and opalescent. Neutron scattering specimens were sealed between two pieces of $\frac{1}{16}$-in.-thick optical quality quartz disks using Viton O rings.

SANS experiments were performed at the National Center for Small Angle Scattering Research (Oak Ridge National Laboratory) with 4.75-Å wavelength neutrons. Three different detector settings were used allowing data collection over the following ranges of wave vector q: $0.079 \text{ Å}^{-1} \leq q \leq 0.2 \text{ Å}^{-1}$ (2.6 m); $0.009 \text{ Å}^{-1} \leq q \leq 0.077 \text{ Å}^{-1}$ (6.91 m); $0.003 \text{ Å}^{-1} \leq q \leq 0.028 \text{ Å}^{-1}$ (19 m). The scattered neutrons were counted with a two-dimensional position-sensitive area detector, and subsequently corrected for cell scattering, detector sensitivity,

sample thickness (typically 2.2 mm), and converted into absolute units according to procedures described elsewhere.[17]

Figure 1 shows a plot of the intensity scattered by dry Vycor as a function of the momentum transfer q. The good agreement of the data obtained for the three different detector settings, which have been spliced together without any adjustment of the intensity scale, demonstrates the satisfactory performance of the calibration procedures. The dominant feature is a broad peak centered around $q = 0.023 \text{ Å}^{-1}$. This is reminiscent of the structure factors measured on two-component systems that underwent spinodal demixing. A simple formulation of such phenomena has been given by Cahn.[18] This model predicts the wave-vector dependence of the scattered in-
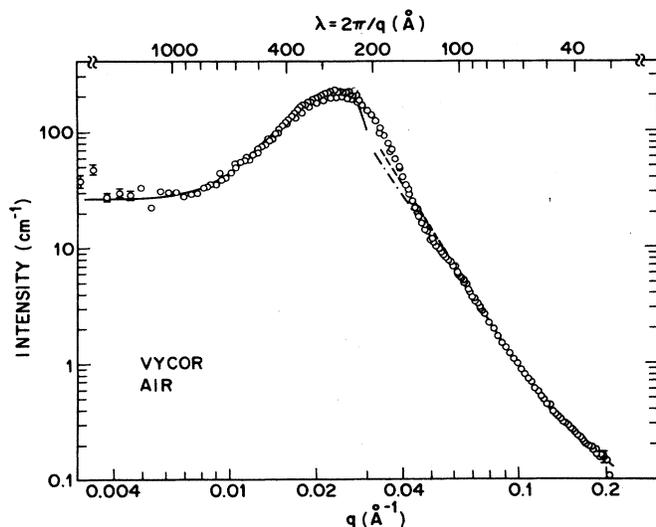
FIG. 1. Intensity of neutrons scattered by dry Vycor as a function of momentum transfer q. Three data sets obtained for various detector settings are spliced together. Statistical error bars are smaller than the symbol if not indicated. The solid line is a fit to the Cahn prediction Eq. (1). The dashed and dashed-dotted lines are fits to Eq. (2) (see text).

tensity as a function of time after a binary system has been quenched into the unstable spinodal regime to evolve as

$$I(\bar{q},\bar{\tau}) = \frac{I(0,0)}{1+\bar{q}^2} \exp[-2\bar{q}^2\bar{\tau}(-1+\bar{q}^2)] \ , \qquad (1)$$

where $\bar{q} = q\lambda/2\pi$ is a dimensionless wave vector involving the wavelength of composition fluctuations λ. $\bar{\tau}$ is the time in dimensionless units evolved since the quench.

Concentrating on the long-wave-length behavior, first we show in Fig. 1 a three-parameter fit of Eq. (1) to the data for $q \leq 0.028$ Å^{-1}. Besides an amplitude, which is uninteresting in this context, the solid line in Fig. 1 corresponds to $\lambda = 192$ Å and $\bar{\tau} = 5.7$. Note that Eq. (1) has a maximum at $\bar{q} = 1/\sqrt{2}$, yielding $q_{max} = 0.023$ Å^{-1}. Since neither the diffusion coefficient of the glass melt nor the real time evolved after quenching are known, $\bar{\tau}$ cannot be further evaluated. We note, however, that $\bar{\tau}$ is small enough to justify the use of the linear theory result [Eq. (1)] which is only valid for early-stage spinodal decomposition. The fact that our data are in good agreement with the Cahn model shows that the leaching process does not alter the long-wave-length structure established by the decomposition process.

For high q the scattering derives mostly from the internal interfaces. In the case of surfaces characterized by a fractal dimension d_s the following asymptotic q dependence has been derived:[19]

$$I(q) = aq^{d_s - 6} \ . \qquad (2)$$

This correctly gives the classical Porod exponent[20] of -4 for sharp boundaries with $d_s = 2$. Recently, Schaefer, Bunker, and Wilcoxon[21] have proposed that $d_s = 2$ for porous Vycor glass, based on small-angle neutron and x-ray scattering data. Three-parameter fits to our SANS results, allowing for a small background b caused by incoherently scattered neutrons, show that the amplitude a and the exponent in Eq. (2) are highly correlated. The data for $q > 0.05$ Å^{-1} yield $a = 1.53 \times 10^{-4}$, $d_s = 2.21$, and $b = 0.07$ (dashed-dotted line in Fig. 1). However, an almost equally good fit (dashed line in Fig. 1) is obtained for $a = 8.32 \times 10^{-5}$ and $b = 0.129$ with d_s fixed at 2. Unfortunately, it is impossible to independently discriminate between these two background levels, and we must conclude that on the basis of the data in Fig. 1 alone it is impossible to decide whether the internal surfaces are rough or not.

In order to study the internal structure in more detail we changed the scattering contrast by imbibing Vycor with protonated (C_6H_{12}) and deuterated (C_6D_{12}) cyclohexane. In general, the intensity scattered by an object composed of two different uniform substances, filling fractions ϕ_1 and ϕ_2 of the total volume, is related to the structure factor $S(q)$ of the object by

$$I(q) \propto (\rho_1 - \rho_2)^2 S(q) \ , \qquad (3)$$

where ρ_1 and ρ_2 are the uniform scattering-length densities of substances 1 and 2, respectively. It can be seen in Fig. 2 that a 50/50 mixture by volume of C_6H_{12} and C_6D_{12} nearly completely contrast matches Vycor, reducing the intensity scattered at $q = 0.023$ Å^{-1} by a factor of
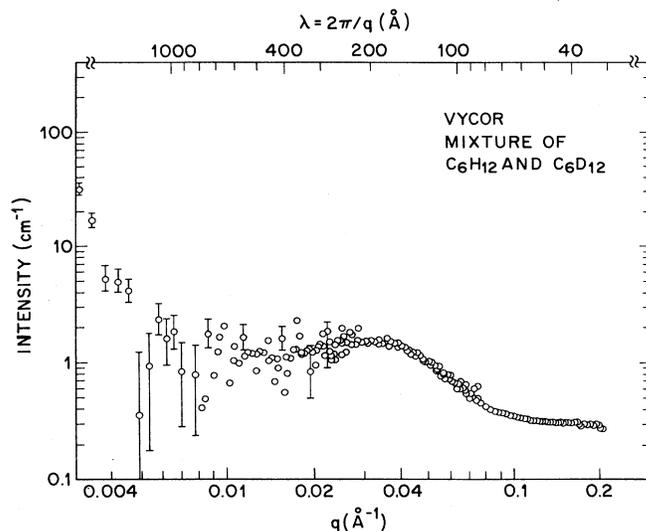
FIG. 2. Intensity of neutrons scattered by Vycor imbibed with a 50/50 mixture by volume of C_6H_{12} and C_6D_{12}.

about 200. A significant feature of Fig. 2 is that the residual weak scattering peak, resulting from incomplete contrast matching has shifted to approximately 0.035 Å^{-1}. Similarly we determined the ratio of neutrons scattered by dry Vycor, and Vycor imbibed with C_6H_{12} or C_6D_{12} (Fig. 3) to be 0.85 and 1.13, respectively, in the long-wave-length region $q \leq 0.035$ Å^{-1}. We emphasize that these ratios are q independent only for low q, i.e., long-wave-length fluctuations. From the known scattering-length densities $\rho_{C_6H_{12}} = -2.77 \times 10^9$ cm^{-2} and $\rho_{C_6D_{12}} = 6.69 \times 10^{10}$ cm^{-2} we can thus calculate $\rho_{Vycor} = 3.35 \pm 0.13 \times 10^{10}$ cm^{-2}. This value is in close agreement with that calculated for amorphous silica $\rho_{SiO_2} = 3.5 \times 10^{10}$ cm^{-2}.

A direct comparison of the intensity scattered by Vycor contrasted in three different ways in the high-q regime is also shown in Fig. 3. We observe the absence of simple power-law behavior in the data around $q = 0.05$ Å^{-1} for
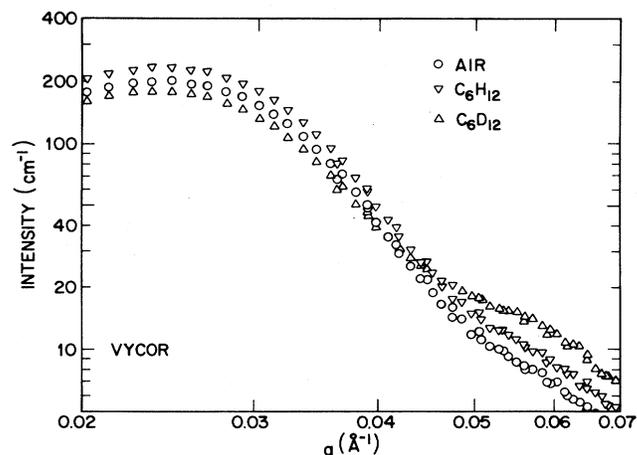
FIG. 3. Intensity of neutrons scattered by Vycor contrasted with air, protonated and deuterated cyclohexane.

STRUCTURE OF POROUS VYCOR GLASS

all three data sets. In addition, we surprisingly observe a crossover in the data. There are two possible explanations for this behavior. Either there are local gradients in the scattering density within the fluid or local gradients within the glass. The former might be expected for binary fluid mixtures with dissimilar wetting properties. This explanation seems unlikely, however, for a mixture of the chemically very similar C_6H_{12} and C_6D_{12}, and is inconceivable for the one fluid (C_6H_{12} or C_6D_{12}) samples. We are thus led to conclude that the high-q data reveal composition gradients within the glass.

A schematic one-dimensional model that qualitatively explains the crossover behavior in Fig. 3 is depicted in Fig. 4. The top half shows the (hypothetical) dominant Fourier component of the scattering-length density of the spinodally decomposed glass; the strict periodicity is an obvious oversimplification and has been chosen for reasons of simplicity. The etching solvent will attack the regions poor in SiO_2, which are the valleys if we assume, for the sake of the argument, that ρ is proportional to the concentration of SiO_2. After the solvent and solute have been removed, the now porous glass can be filled with appropriate fluids, as depicted in the bottom half of Fig. 4. Note that at early stages of spinodal decomposition one expects a structure with significant spatial nonuniformity rather than fully phase-separated domains with steep composition profiles as occurs in later, coarsened stages. The bottom half of Fig. 4 readily reveals two qualitative features observed in Fig. 3. First, the dominant Fourier component ($\lambda = 272$ Å) has a smaller amplitude when contrasted with C_6D_{12} than with C_6H_{12}, leading to a smaller scattered intensity in the former case at that particular wave vector (see Fig. 3 at $q = 0.025$ Å^{-1}). Secondly, higher-frequency components are in phase for the deuterated case, leading to a higher amplitude for those composition fluctuations and, thus, a larger scattered intensity in the high-q regime. For similar reasons, perfect contrast matching should be impossible. Furthermore, owing to the q dependence of the effective contrast (Fig. 3) the measured main peak location will depend somewhat on the scattering-length density of the imbibed fluid, particularly when near the optimal contrast matching condition. These observations are consistent with the results shown in Figs. 1 and 2.

Since the scattered intensity is known in absolute units and $d_s \approx 2$ we apply Porod's law in the high-q regime to determine the surface-to-volume ratio S/V of the scattering sample

$$I(q) = \frac{S}{V} 2\pi \frac{(\rho_{Vycor} - \rho_{liquid})^2}{q^4}, \qquad (4)$$

where ρ_{liquid} is the scattering-length density of either C_6H_{12} or C_6D_{12}. S/V determined for C_6H_{12} and C_6D_2 contrast yield 121 m^2/cm^3 and 185 m^2/cm^3, respectively. The discrepancy between these two values further corroborates the concept of spatial nonuniformity of the glass density, leading to the failure of Eq. (4), which is valid only for the two-phase model with domains of constant ρ. Further support for this view is provided by the results of
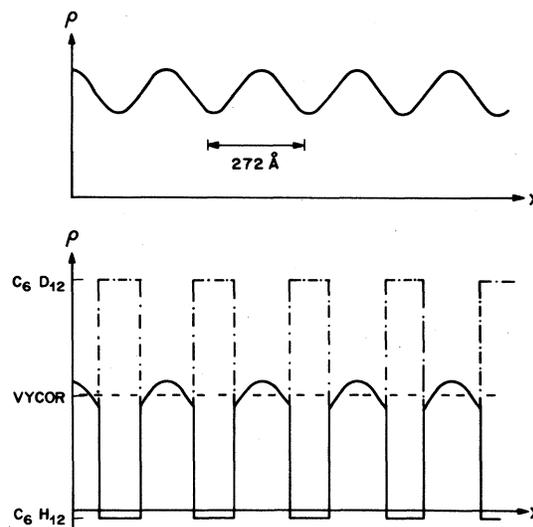
FIG. 4. One-dimensional schematic model for early-stage spinodal decomposition. The top half represent the spatial scattering density fluctuations before coarsening could occur. Etching attacks, e.g., regions of low-density ρ, which subsequently can be filled with appropriate fluids producing density profiles as indicated by the C_6H_{12} and C_6D_{12} lines.

Brunauer-Emmett-Teller (BET) adsorption isotherm measurements, which yield $S/V = 157$ m^2/cm^3, which is very close to the mean of the above values.

We conclude that the structure of Vycor has the long-wave-length characteristics of a spinodally decomposed binary system at its early stages. The high-q data of our SANS experiments *do not* allow us to make definitive statements about the roughness of the internal surfaces. Experiments in which the scattering contrast has been varied reveal local composition gradients within the glass which complicate determination of the fractal dimensionality of the surfaces. These features also create pitfalls for S/V determination by Porod analysis and must be taken into account in the analysis of scattering data of more complicated systems, e.g., binary fluid mixtures imbibed in Vycor.

Note added. N. F. Berk very recently proposed[22] a model describing the scattering properties of microdispersed and microporous systems. A significant prediction of this model is higher-order harmonics in the scattering intensity, in qualitative agreement with the large-q data we have presented.

[1]L. de Arcangelis, J. Koplik, S. Redner, and D. Wilkinson, Phys. Rev. Lett. **57**, 996 (1986); D. Wilkinson and J. F. Willemsen, J. Phys. A **16**, 3365 (1983); D. Wilkinson, Phys. Rev. A **30**, 520 (1984).

[2]E. Guyon, in *On Growth and Form,* edited by H. E. Stanley and N. Ostrowsky (Martinus Nijhoff, Hingham, MA, 1986).

[3]R. Lenormand and C. Zarcone, Phys. Rev. Lett. **54**, 2226 (1985).

[4]J. Willemsen, in *On Growth and Form,* edited by H. E. Stanley and N. Ostrowsky (Martinus Nijhoff, Hingham, MA, 1986).

[5]J. D. Chen and D. Wilkinson, Phys. Rev. Lett. **55**, 1892 (1985).

[6]J. P. Stokes, D. A. Weitz, J. P. Gollub, A. Dougherty, M. O. Robbins, P. M. Chaikin, and H. M. Lindsay, Phys. Rev. Lett. **57**, 1718 (1986).

[7]W. D. Dozier, J. M. Drake, and J. Klafter, Phys. Rev. Lett. **56**, 197 (1986).

[8]M. T. Bishop, K. H. Langley, and F. E. Karasz, Phys. Rev. Lett. **57**, 1741 (1986).

[9]D. D. Awschalom, J. Warnock, and M. W. Shafer, Phys. Rev. Lett. **57**, 1607 (1986); J. Warnock, D. D. Awschalom, and M. W. Shafer, *ibid.* **57**, 1753 (1986).

[10]U. Even, K. Rademann, J. Jortner, N. Manor, and R. Reisfeld, Phys. Rev. Lett. **52**, 2164 (1984).

[11]R. Kopelman, S. Parus, and J. Prasad, Phys. Rev. Lett. **56**, 1742 (1986).

[12]P. Levitz and J. M. Drake, Phys. Rev. Lett. **58**, 686 (1987).

[13]B. C. Crooker, B. Hebral, E. N. Smith, Y. Takano, and J. D. Reppy, Phys. Rev. Lett. **51**, 666 (1983).

[14]M. Rasolt, M. J. Stephen, M. E. Fisher, and P. B. Weichmann, Phys. Rev. Lett. **53**, 798 (1984).

[15]M. C. Goh, W. I. Goldburg, and C. M. Knobler, Phys. Rev. Lett. **58**, 1008 (1987).

[16]S. B. Dierker and P. Wiltzius, Phys. Rev. Lett. **58**, 1865 (1987).

[17]G. D. Wignall and F. S. Bates, J. Appl. Crystallogr. **20**, 28 (1987).

[18]J. W. Cahn, Acta Metall. **9**, 795 (1961).

[19]H. D. Bale and P. W. Schmidt, Phys. Rev. Lett. **53**, 596 (1984).

[20]See, e.g., G. Porod, in *Small Angle X-ray Scattering,* edited by Otto Glatter and H. C. Kratky (Academic, New York, 1982).

[21]D. W. Schaefer, B. C. Bunker, and J. P. Wilcoxon, Phys. Rev. Lett. **58**, 284 (1987).

[22]N. F. Berk, Phys. Rev. Lett. **58**, 2718 (1987).